



Crystal structure of betaine aldehyde dehydrogenase from *Burkholderia pseudomallei*

Dylan K. Beard,^a Sandhya Subramanian,^{b,c} Jan Abendroth,^{c,d} David M. Dranow,^d Thomas E. Edwards,^{c,d} Peter J. Myler^{b,c,e} and Oluwatoyin A. Asojo^{a*}

^aDepartment of Chemistry and Biochemistry, Hampton University, 100 William R. Harvey Way, Hampton, VA 23668, USA, ^bCenter for Global Infectious Disease Research, Seattle Children's Research Institute, 307 Westlake Avenue North Suite 500, Seattle, WA 98109, USA, ^cSeattle Structural Genomics Center for Infectious Disease (SSGCID), Seattle, Washington, USA, ^dUCB-Bainbridge, Bainbridge Island, WA 98110, USA, and ^eDepartment of Global Health and Department of Biomedical Informatics and Medical Education, University of Washington, Seattle, WA 98195, USA. *Correspondence e-mail: oluwatoyin.asojo@hamptonu.edu

Received 1 November 2021

Accepted 19 December 2021

Edited by F. T. Tsai, Baylor College of Medicine, Houston, USA

Keywords: *Burkholderia pseudomallei*; melioidosis; disulfiram; betaine aldehyde dehydrogenase; inhibition; drug repurposing.

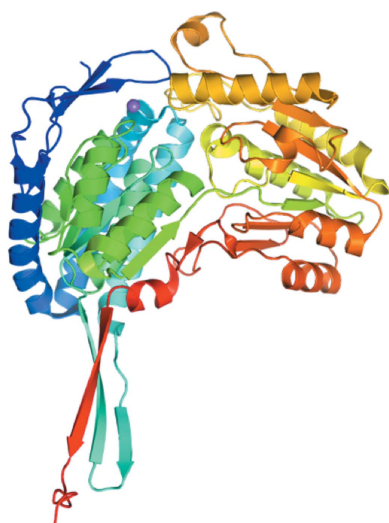
PDB references: betaine aldehyde dehydrogenase, 6wsa; bound to cofactor, 6wsb

Supporting information: this article has supporting information at journals.iucr.org/f

Burkholderia pseudomallei infection causes melioidosis, which is often fatal if untreated. There is a need to develop new and more effective treatments for melioidosis. This study reports apo and cofactor-bound crystal structures of the potential drug target betaine aldehyde dehydrogenase (BADH) from *B. pseudomallei*. A structural comparison identified similarities to BADH from *Pseudomonas aeruginosa* which is inhibited by the drug disulfiram. This preliminary analysis could facilitate drug-repurposing studies for *B. pseudomallei*.

1. Introduction

Burkholderia pseudomallei is a rod-shaped, motile, flagellated, soil-dwelling Gram-negative proteobacterium of the Burkholderiaceae family that thrives in tropical and subtropical regions (Gassiep *et al.*, 2021). *B. pseudomallei* causes melioidosis, a deadly emerging opportunistic infection mainly of the immunocompromised (Hall *et al.*, 2019; Poe *et al.*, 1971; Veluthat *et al.*, 2021). *B. pseudomallei* is transmitted through open wounds, contact with contaminated soil and water, ingestion or inhalation, and it is also a potential biological warfare agent (Goarant *et al.*, 2021). Melioidosis is endemic in South Asia and Northern Australia, with ~165 000 cases annually; however, the global distribution of *B. pseudomallei* is unknown, as the associated disease is underreported and misdiagnosed (Patil *et al.*, 2016; Poe *et al.*, 1971; Veluthat *et al.*, 2021). Typically, about 12 cases of melioidosis are reported annually in mainland USA, and most patients had traveled internationally; however, *B. pseudomallei* occurs naturally in Puerto Rico and the US Virgin Islands (Hall *et al.*, 2019). Melioidosis symptoms include localized pain and swelling, ulcer, cough, headache, anorexia, joint pain, brain infection, seizures, fever, pneumonia, low blood pressure and abscesses (Hall *et al.*, 2019; Poe *et al.*, 1971; Veluthat *et al.*, 2021). Thus, melioidosis may be misdiagnosed as tuberculosis, pneumonia or other diseases (Veluthat *et al.*, 2021). Symptoms may appear a few days or several years after exposure, and the mortality rate of untreated melioidosis is around 90% (Loveleena *et al.*, 2004; Patil *et al.*, 2016; Poe *et al.*, 1971; Veluthat *et al.*, 2021). Melioidosis is currently treated with two to eight weeks of intravenous antimicrobial therapy (ceftazidime or meropenem) followed by 3–6 months of oral antimicrobial therapy (amoxicillin/clavulanic acid or trimethoprim–sulfamethoxazole),



OPEN ACCESS

but still results in ~40% mortality (Fen *et al.*, 2021). As a part of efforts to develop new therapeutics and diagnostics for melioidosis, the Seattle Structural Genomics Center for Infectious Disease (SSGCID) has determined the crystal structure of betaine aldehyde dehydrogenase (BADH) from *B. pseudomallei* (*BpBADH*). BADH catalyzes the irreversible oxidation of betaine aldehyde to the osmoprotectant betaine and is being investigated as a drug target for drug-resistant bacteria, notably *Pseudomonas aeruginosa*, because its inhibition blocks choline catabolism and leads to the accumulation of the highly toxic betaine aldehyde (González-Segura *et al.*, 2009).

2. Materials and methods

2.1. Production of *BpBADH*

Cloning, expression and purification were conducted as part of the Seattle Structural Genomics Center for Infectious Disease (SSGCID; Myler *et al.*, 2009; Stacy *et al.*, 2011) following standard protocols as described previously (Bryan *et al.*, 2011; Choi *et al.*, 2011; Serbzhinskiy *et al.*, 2015). The full-length betaine aldehyde dehydrogenase gene from *B. pseudomallei* (*BpBADH*; UniProt Q3JLL8) encoding amino acids 1–489 was PCR-amplified from genomic DNA using the primers shown in Table 1.

The gene was cloned into the ligation-independent cloning (LIC; Aslanidis & de Jong, 1990) expression vector pMCSG26 (Eschenfeldt *et al.*, 2010) encoding a noncleavable C-terminal 6×His fusion tag (ORF-GHHHHHH). Plasmid DNA was transformed into chemically competent *Escherichia coli* BL21(DE3)R3 Rosetta cells. The plasmid containing Q3JLL8 was expression-tested, and 2 l of culture was grown using auto-induction medium (Studier, 2005) in a LEX Bioreactor (Epiphyte Three Inc.) as described previously (Serbzhinskiy *et al.*, 2015). The expression clone BupsA.00020.b.AE1.GE43326 is available at <https://www.ssgcid.org/available-materials/expression-clones/>.

BpBADH-His was purified using a two-step protocol consisting of an immobilized metal-affinity chromatography (IMAC) step and size-exclusion chromatography (SEC). All chromatography runs were performed on an ÄKTApurifier 10 (GE) using automated IMAC and SEC programs according to previously described procedures (Bryan *et al.*, 2011). Thawed bacterial pellets were lysed by sonication in 200 ml lysis buffer [25 mM 4-(2-hydroxyethyl)-1-piperazineethanesulfonic acid (HEPES) pH 7.0, 500 mM NaCl, 5% glycerol, 0.5% 3-[(3-cholamidopropyl)dimethylammonio]-1-propanesulfonate (CHAPS), 30 mM imidazole, 10 mM MgCl₂, 1 mM tris(2-carboxyethyl)phosphine hydrochloride (TCEP), 250 µg ml⁻¹ 4-(2-aminoethyl)benzenesulfonyl fluoride hydrochloride (AEBSF), 0.025% sodium azide]. After sonication, the crude lysate was clarified with 20 µl (25 units µl⁻¹) Benzonase and incubated while mixing at room temperature for 45 min. The lysate was clarified by centrifugation at 10 000 rev min⁻¹ for 1 h using a Sorvall centrifuge (Thermo Scientific). For the IMAC step, the clarified supernatant was passed over an

Table 1
Macromolecule-production information.

Source organism	<i>Burkholderia pseudomallei</i> 1710b
DNA source	Dr Samuel I. Miller, University of Washington, USA
Forward primer	5'-ATGTCGGTATACGGTCTGCAGC-3'
Reverse primer	5'-GAACACCGGTTGATAGCGGCC-3'
Expression vector	pMCSG26
Expression host	<i>E. coli</i> BL21(DE3)R3 Rosetta cells
Complete amino-acid sequence of the construct produced	MSVYGLQRLYIAGAHADATSGKTFDFTDPATGELLARVQQASADDVDRAVASAREGQR EWAAMTAMQRSRILRRAVELLRRNDAL AELEMRDTGKPIAETRAVDIVTGADVIE YYAGLATAIEGLQVPLRPESFVYTRREP LGVCAGIGAWNYPIQIACWKSAPALAAG NAMIFKPESEVTPLSALKLAEIYTEAGVP AGVFNVVQGDGSGVALLSAHPGIKVSF TGGVETGKKVMSLAGASSLKEVTMELGG KSPILVFDADLDRAADIAVTANFFSAG QVCTNGTRVVFVQAVKDAFVERVLARVA RIRVGKPSDSTNFGPLASAAQDKVLG YIDSGKAEGAKLLAGGARLVNDHFASGQ YVAPTVFGDCRDDMRIVREEIFGPVMSI LSFETEDEATARANATDYGLAAGVVTEN LSRAHRAIHRLEAGICWINTWGESP AEM PVGGYKQSGVGRENGITTL EHYTRIKSV QVELGRYQVFGHHHHH

Ni-NTA HisTrap FF 5 ml column (GE Healthcare) which had been pre-equilibrated with loading buffer (25 mM HEPES pH 7.0, 500 mM NaCl, 5% glycerol, 30 mM imidazole, 1 mM TCEP, 0.025% sodium azide). The column was washed with 20 column volumes (CV) of loading buffer and was eluted with loading buffer and 250 mM imidazole in a linear gradient over 7 CV. Peak fractions, as determined by UV absorbance at 280 nm, were pooled and concentrated using an Amicon concentrator to a volume of 5 ml for SEC. For SEC, a SEC column (Superdex 75, GE) was equilibrated with running buffer [25 mM HEPES pH 7.0, 500 mM NaCl, 5% glycerol, 2 mM dithiothreitol (DTT), 0.025% sodium azide]. The eluted peak fractions were collected and analyzed for the presence of *BpBADH* by SDS-PAGE. The SEC peak fractions containing *BpBADH* eluted as a single large peak at a molecular mass of ~77 kDa. A dimer of *BpBADH* is expected to have a molecular mass of ~106 kDa, while a monomer has a molecular mass of ~53 kDa. *BpBADH* may be a monomer in the absence of a cofactor, while it dimerizes in the presence of the cofactor or other ligands. Further biophysical analysis is required to determine whether *BpBADH* dimerizes in the presence of NAD in solution. Interestingly, the dimer has been reported in more than 175 reported BADH structures with ligands, cofactors and inhibitors in the PDB and is consistent with the observed crystal form of *BpBADH* with NAD (Fig. 1).

The peak fractions were pooled and concentrated to 34.72 mg ml⁻¹ using an Amicon concentrator (Millipore). The protein concentration was assessed using the OD₂₈₀ and a molar extinction coefficient of 46 870 M⁻¹ cm⁻¹. Purified protein was aliquoted into 200 µl aliquots, flash-frozen in liquid nitrogen and stored at -80°C until use for crystallization. The purified protein (batch BupsA.00020.b.AE1.PS38619) is available at <https://www.ssgcid.org/available-materials/ssgcid-proteins/>.

Table 2
Crystallization.

Method	Sitting-drop vapor diffusion
Plate type	96-well Compact 300, Rigaku
Temperature (K)	287
Protein concentration (mg ml ⁻¹)	34.72
Buffer composition of protein solution	
Apo crystals	25 mM HEPES pH 7.0, 500 mM NaCl, 5% glycerol, 2 mM DTT, 0.025% azide
NAD-bound crystals	25 mM HEPES pH 7.0, 500 mM NaCl, 5% glycerol, 2 mM DTT, 0.025% azide, 4 mM NAD
Composition of reservoir solution	
Apo structure	JCSG+ condition F7: 0.8 M succinate pH 7.0
NAD-bound structure	Morpheus condition H11: 10% PEG 4000, 20% glycerol, 0.02 M sodium L-glutamate, 0.02 M DL-alanine, 0.02 M glycine, 0.02 M DL-lysine, 0.02 M DL-serine, 0.1 M bicine/Trizma pH 8.5
Volume and ratio of drop	0.4 µl protein plus 0.4 µl reservoir
Volume of reservoir (µl)	80
Cryoprotectant	20% ethylene glycol

2.2. Crystallization

Purified *Bp*BADH-His was screened for crystallization in 96-well sitting-drop plates against the JCSG++ HTS (Jena Bioscience), MCSG1 (Molecular Dimensions) and Morpheus (Rigaku Reagents; Gorrec, 2009, 2015) crystal screens. The protein solution for the apo structure did not contain NAD, whereas 4 mM NAD was added to the protein solution for the NAD-bound complex (Table 2). Equal volumes of protein solution (0.4 µl) and precipitant solution were set up at 287 K

Table 3
Data collection and processing.

Values in parentheses are for the outer shell.

PDB code	6wsa	6wsb
Ligand	—	NAD
Diffraction source	21-ID-F, APS	21-ID-F, APS
Wavelength (Å)	0.97872	0.97872
Temperature (K)	100	100
Detector	RayoniX MX300HE CCD	RayoniX MX300HE CCD
Crystal-to-detector distance (mm)	270	200
Rotation range per image (°)	1	1
Total rotation range (°)	60	150
Space group	<i>P</i> 6 ₂ 22	<i>P</i> 2 ₁ 2 ₁ 2
<i>a</i> , <i>b</i> , <i>c</i> (Å)	107.86, 107.86, 233.53	99.27, 156.70, 76.23
α , β , γ (°)	90, 90, 120	90, 90, 90
Mosaicity (°)	0.143	0.103
Resolution range (Å)	49.51–2.05 (2.10–2.05)	43.09–1.55 (1.59–1.55)
Total No. of reflections	362438 (26952)	1054995 (75766)
No. of unique reflections	51154 (3702)	172302 (12622)
Completeness (%)	99.9 (99.9)	99.9 (100.0)
Multiplicity	7.09 (7.28)	6.12 (6.00)
$\langle I/\sigma(I) \rangle$	12.86 (3.50)	16.47 (3.02)
$R_{r.i.m.}$	0.101 (0.548)	0.083 (0.621)
Overall <i>B</i> factor from Wilson plot (Å ²)	32.748	20.398

against reservoir (80 µl) in sitting-drop vapor-diffusion format. The final crystallization precipitant was JCSG+ condition F7 for the apo form and Morpheus condition H11 for the NAD-bound form (see Table 2). After cryoprotectant exchange into crystallization solution supplemented with 20% ethylene

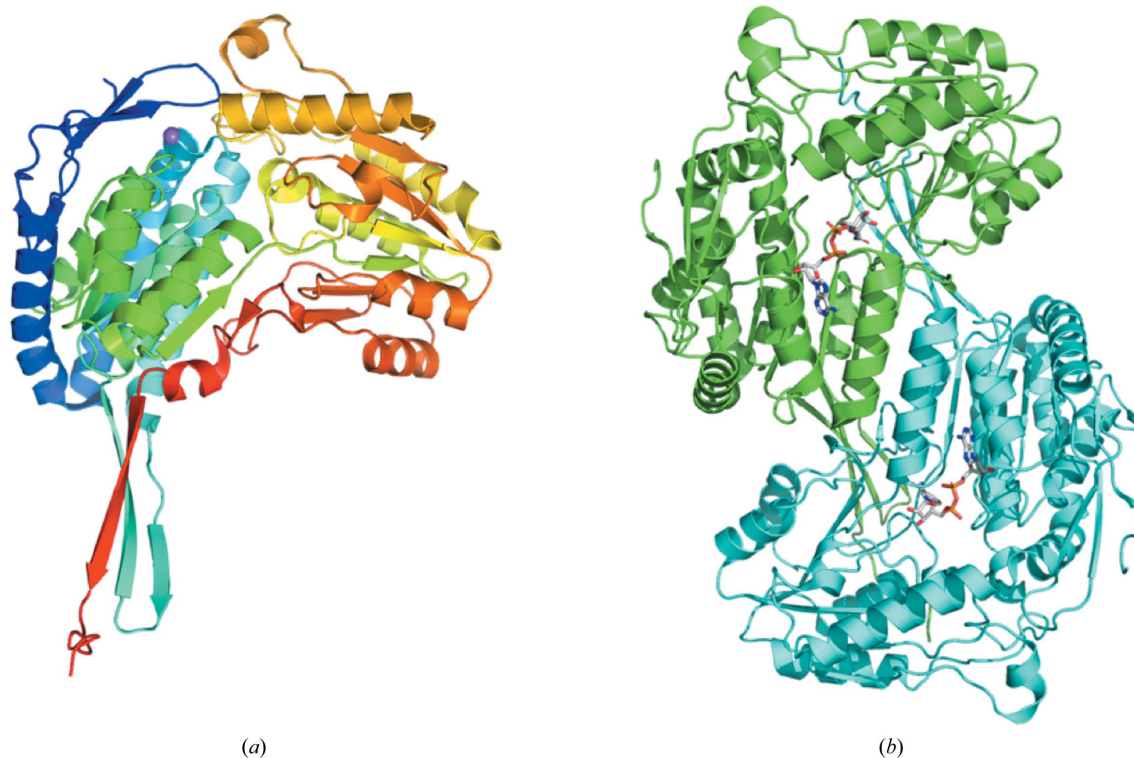


Figure 1

Structure of *B. pseudomallei* betaine aldehyde dehydrogenase (*Bp*BADH). (a) Monomer of apo *Bp*BADH (rainbow colored from blue at the N-terminus to red at the C-terminus). (b) Dimer of *Bp*BADH with NAD (monomers are shown as aquamarine and cyan ribbons, with NAD shown as sticks).

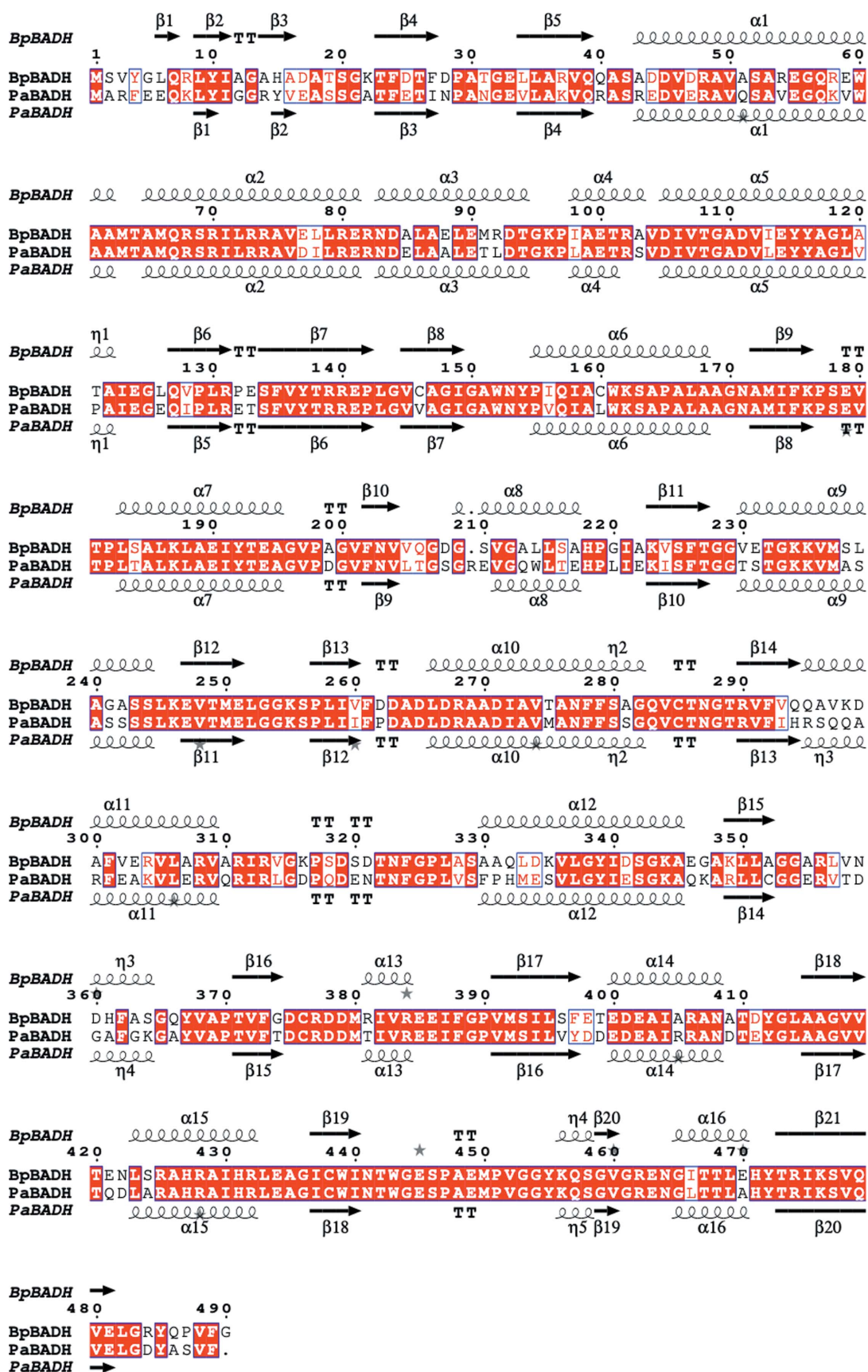


Figure 2 Structural and primary-sequence alignment of *BpBADH* and *PaBADH*. The secondary-structure elements shown are α -helices (α), 3_{10} -helices (η), β -strands (β) and β -turns (TT). Identical residues are shown in white on a red background and conserved residues are shown in red.

Table 4
Structure solution and refinement.

Values in parentheses are for the outer shell.

PDB code	6wsa	6wsb
Ligand	Glycerol	NAD
Resolution range (Å)	49.51–2.05 (2.08–2.05)	43.09–1.55 (1.57–1.55)
Completeness (%)	96.1	96.4
σ Cutoff	$F > 0.000\sigma(F)$	$F > 0.000\sigma(F)$
No. of reflections, working set	49171 (1957)	166209 (4765)
No. of reflections, test set	2932 (109)	10050 (297)
Final R_{cryst}	0.140 (0.2203)	0.144 (0.2064)
Final R_{free}	0.173 (0.2521)	0.169 (0.2342)
Cruickshank DPI	0.183	0.070
No. of non-H atoms		
Protein	3666	7322
Ion	1	—
Ligand	60	100
Solvent	501	1388
Total	4228	8810
R.m.s. deviations		
Bond lengths (Å)	0.006	0.006
Angles (°)	0.775	0.85
Average B factors (Å ²)		
Protein	33.0	15.3
Ion	32.1	—
Ligand	58.9	31.7
Water	42.6	30.8
Ramachandran plot		
Most favored (%)	97.1	97.1
Allowed (%)	2.9	2.9

glycol, the crystals were harvested and flash-cooled by plunging them into liquid nitrogen.

2.3. Data collection and processing

Data were collected at 100 K on beamline 21-ID-F at the Advanced Photon Source (APS), Argonne National Laboratory (see Table 3). Data sets were reduced with *XSCALE* (Kabsch, 2010). Raw X-ray diffraction images are available from the Integrated Resource for Reproducibility in Macromolecular Crystallography at <https://www.proteindiffraction.org/>.

2.4. Structure solution and refinement

The structures were solved by molecular replacement with *Phaser* (McCoy *et al.*, 2007) from the *CCP4* suite of programs (Collaborative Computational Project, Number 4, 1994; Krissinel *et al.*, 2004; Winn *et al.*, 2011) using PDB entry 2wox (Díaz-Sánchez *et al.*, 2011) as the search model. The structure was refined using iterative cycles of *Phenix* (Liebschner *et al.*, 2019) followed by manual rebuilding of the structure using *Coot* (Emsley & Cowtan, 2004; Emsley *et al.*, 2010). The quality of both structures was checked using *MolProbity* (Chen *et al.*, 2010). All data-reduction and refinement statistics are shown in Table 4. The structures of apo *BpBADH* and *BpBADH* with NAD were refined to resolutions of 2.05 and

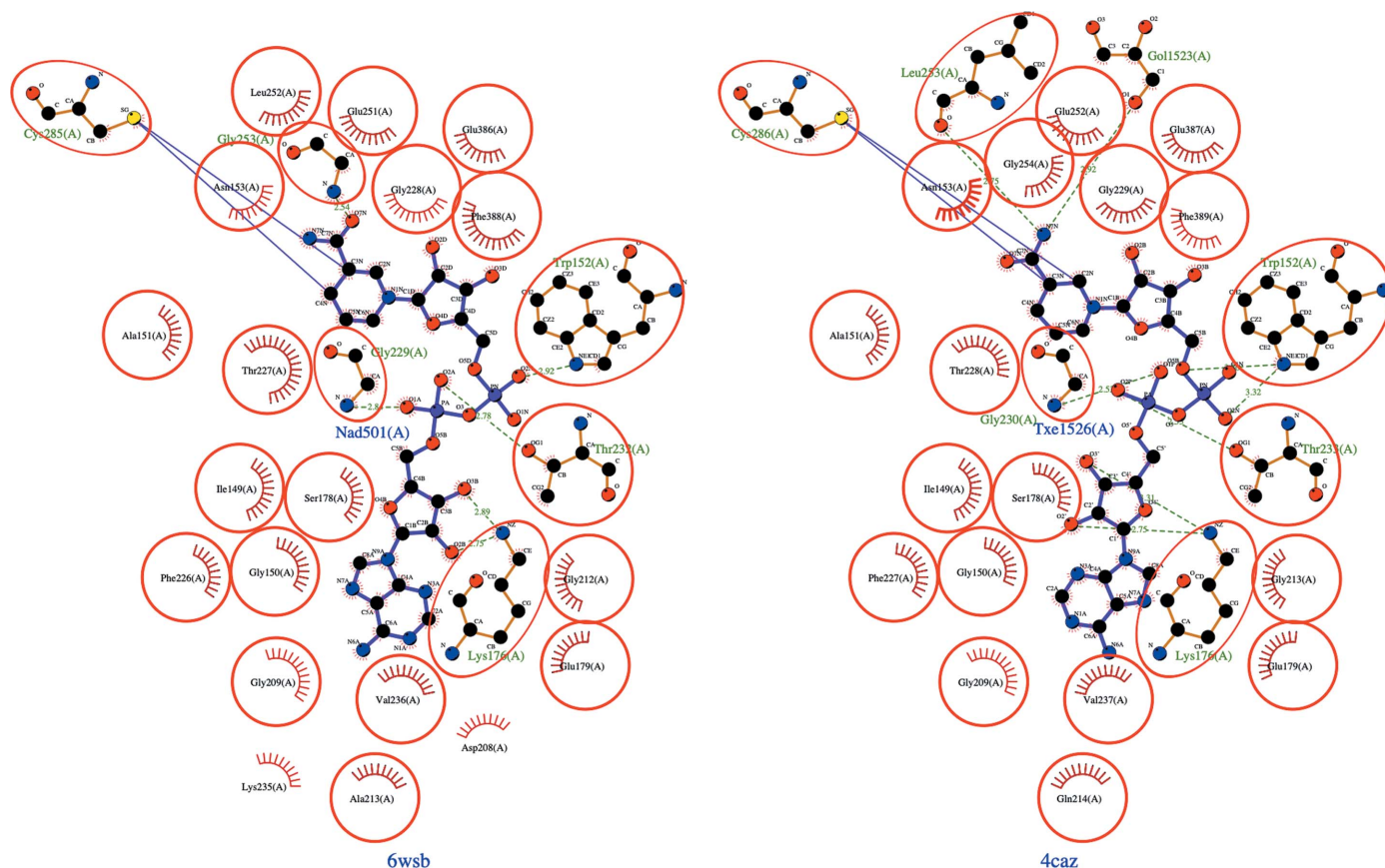


Figure 3
LIGPLOT analysis reveals that the cofactor-binding domains of *BpBADH* (PDB entry 6wsb) and *PaBADH* (PDB entry 4caz) are well conserved (circles indicate identical residues). Both structures show the conserved catalytic cysteine irreversibly inhibited by disulfiram.

1.55 Å, respectively. Structural figures were analyzed and prepared using *PyMOL* (DeLano, 2002). Multiple sequence alignments were generated with *Clustal Omega* (Li *et al.*, 2015). Coordinates and structure factors have been deposited in the Protein Data Bank (<https://www.rcsb.org/>; Berman *et al.*, 2000) with accession numbers 6wsa and 6wsb for apo *BpBADH* and *BpBADH* in complex with NAD, respectively.

3. Results and discussion

The two structures reported here are of apo *BpBADH* and its complex with the cofactor NAD (Fig. 1). The monomers are very similar and have an r.m.s.d. of ~0.17 Å for main-chain atoms. The 489 amino acids in each monomer fold as 20.4% β -strand, 39.3% α -helix, 2.5% 3_{10} -helix and 37.8% loops, forming six β - α - β motifs that contain five β -sheets (four mixed and one antiparallel). The structure also contains 21 helices, 21 strands, four β -hairpins, four β -bulges and 25 helix-helix interactions. *BpBADH* has a prototypical BADH topology and shares considerable structure and sequence similarity with the ortholog from *P. aeruginosa* (*PaBADH*; Fig. 2). The 489-amino-acid sequence of *PaBADH* folds as 19.6% β -strand, 38.2% α -helix, 2.5% 3_{10} -helix and 39.7% loops (Fig. 2).

The structural similarities and motifs associated with the BADHs from both organisms may accelerate drug-discovery efforts. *PaBADH* is known to be inhibited by disulfiram through the catalytic cysteine (Velasco-García *et al.*, 2006); thus, we hypothesize that *BpBADH* will likewise be inhibited by disulfiram. Disulfiram binds irreversibly to Cys286 in *PaBADH*, which is in the highly conserved cofactor-binding cavity of *PaBADH* and *BpBADH*; the corresponding residue is Cys285 in *BpBADH* (Figs. 2 and 3). Disulfiram is an irreversible inhibitor that leads to a buildup of betaine aldehyde, which becomes toxic in bacterial cells. The toxicity in the bacterial cells stops bacterial growth (Velasco-García *et al.*, 2006). Since disulfiram is FDA-approved for treating chronic alcoholism, preliminary studies suggest that it could be repurposed as a lead compound for melioidosis. Furthermore, due to the structural similarity between *PaBADH* and *BpBADH*, the lessons learned in drug discovery for the former could accelerate efforts in addressing melioidosis.

4. Conclusion

The high-resolution structures of betaine aldehyde dehydrogenase from *B. pseudomallei* (*BpBADH*) and *P. aeruginosa* (*PaBADH*) reveal a conserved NAD-dependent topology and structural similarity. Since the key amino-acid residues in inhibitor-binding sites are conserved, the previous studies on *PaBADH* could facilitate the development of small-molecule inhibitors of *BpBADH*.

Acknowledgements

The SSGCID consortium is directed by Dr Peter Myler (principal investigator) and comprises many different scientists working at multiple centers towards determining the

three-dimensional structures of proteins from biodefense organisms and emerging infectious diseases. In particular, we would like to thank the SSGCID cloning, protein-production and X-ray crystallography groups at the Center for Global Infectious Disease Research, the University of Washington and UCB.

Funding information

This work was supported by federal funds from the National Institute of Allergy and Infectious Diseases (NIAID), National Institutes of Health (NIH), Department of Health and Human Services under Contract No. HHSN272201700059C from 1 September 2017. (SSGCID was funded under NIAID Contracts Nos. HHSN272201200025C from 1 September 2012 through 31 August 2017 and HHSN272200700057C from 28 September 2007 through 27 September 2012.) Dylan K. Beard was part of a Hampton University Chemistry Education and Mentorship Course-based Undergraduate Research pilot (HU-ChEM CURES) funded by the NIGMS (award No. 1U01GM138433-01 to OAA).

References

- Aslanidis, C. & de Jong, P. J. (1990). *Nucleic Acids Res.* **18**, 6069–6074.
- Berman, H. M., Westbrook, J., Feng, Z., Gilliland, G., Bhat, T. N., Weissig, H., Shindyalov, I. N. & Bourne, P. E. (2000). *Nucleic Acids Res.* **28**, 235–242.
- Bryan, C. M., Bhandari, J., Napuli, A. J., Leibly, D. J., Choi, R., Kelley, A., Van Voorhis, W. C., Edwards, T. E. & Stewart, L. J. (2011). *Acta Cryst.* **F67**, 1010–1014.
- Chen, V. B., Arendall, W. B., Headd, J. J., Keedy, D. A., Immormino, R. M., Kapral, G. J., Murray, L. W., Richardson, J. S. & Richardson, D. C. (2010). *Acta Cryst.* **D66**, 12–21.
- Choi, R., Kelley, A., Leibly, D., Nakazawa Hewitt, S., Napuli, A. & Van Voorhis, W. (2011). *Acta Cryst.* **F67**, 998–1005.
- Collaborative Computational Project, Number 4 (1994). *Acta Cryst.* **D50**, 760–763.
- DeLano, W. L. (2002). *PyMOL*. <http://www.pymol.org>.
- Díaz-Sánchez, Á. G., González-Segura, L., Rudiño-Piñera, E., Lira-Rocha, A., Torres-Larios, A. & Muñoz-Clares, R. A. (2011). *Biochem. J.* **439**, 443–452.
- Emsley, P. & Cowtan, K. (2004). *Acta Cryst.* **D60**, 2126–2132.
- Emsley, P., Lohkamp, B., Scott, W. G. & Cowtan, K. (2010). *Acta Cryst.* **D66**, 486–501.
- Eschenfeldt, W. H., Maltseva, N., Stols, L., Donnelly, M. I., Gu, M., Nocek, B., Tan, K., Kim, Y. & Joachimiak, A. (2010). *J. Struct. Funct. Genomics*, **11**, 31–39.
- Fen, S. H. Y., Tandhavanant, S., Phunpang, R., Ekcharyawat, P., Saiprom, N., Chewapreecha, C., Seng, R., Thiansukhon, E., Morakot, C., Sangsa, N., Chayangsu, S., Chuananont, S., Tanwisaid, K., Silakun, W., Buasi, N., Chaisuksant, S., Hompleum, T., Chetchotisakd, P., Day, N. P. J., Chantratita, W., Lertmemongkolchai, G., West, T. E. & Chantratita, N. (2021). *Antimicrob. Agents Chemother.* **65**, e02230-20.
- Gassiep, I., Burnard, D., Bauer, M. J., Norton, R. E. & Harris, P. N. (2021). *Future Microbiol.* **16**, 271–288.
- Goarant, C., Dellagi, K. & Picardeau, M. (2021). *Yale J. Biol. Med.* **94**, 351–360.
- González-Segura, L., Rudiño-Piñera, E., Muñoz-Clares, R. A. & Horjales, E. (2009). *J. Mol. Biol.* **385**, 542–557.
- Gorrec, F. (2009). *J. Appl. Cryst.* **42**, 1035–1042.
- Gorrec, F. (2015). *Acta Cryst.* **F71**, 831–837.

- Hall, C. M., Jaramillo, S., Jimenez, R., Stone, N. E., Centner, H., Busch, J. D., Bratsch, N., Roe, C. C., Gee, J. E., Hoffmaster, A. R., Rivera-Garcia, S., Soltero, F., Ryff, K., Perez-Padilla, J., Keim, P., Sahl, J. W. & Wagner, D. M. (2019). *PLoS Negl. Trop. Dis.* **13**, e0007727.
- Kabsch, W. (2010). *Acta Cryst.* **D66**, 125–132.
- Krissinel, E. B., Winn, M. D., Ballard, C. C., Ashton, A. W., Patel, P., Potterton, E. A., McNicholas, S. J., Cowtan, K. D. & Emsley, P. (2004). *Acta Cryst.* **D60**, 2250–2255.
- Li, W., Cowley, A., Uludag, M., Gur, T., McWilliam, H., Squizzato, S., Park, Y. M., Buso, N. & Lopez, R. (2015). *Nucleic Acids Res.* **43**, W580–W584.
- Liebschner, D., Afonine, P. V., Baker, M. L., Bunkóczi, G., Chen, V. B., Croll, T. I., Hintze, B., Hung, L.-W., Jain, S., McCoy, A. J., Moriarty, N. W., Oeffner, R. D., Poon, B. K., Prisant, M. G., Read, R. J., Richardson, J. S., Richardson, D. C., Sammito, M. D., Sobolev, O. V., Stockwell, D. H., Terwilliger, T. C., Urzhumtsev, A. G., Videau, L. L., Williams, C. J. & Adams, P. D. (2019). *Acta Cryst.* **D75**, 861–877.
- Loveleena, Chaudhry, R. & Dhawan, B. (2004). *J. Assoc. Physicians India*, **52**, 417–420.
- McCoy, A. J., Grosse-Kunstleve, R. W., Adams, P. D., Winn, M. D., Storoni, L. C. & Read, R. J. (2007). *J. Appl. Cryst.* **40**, 658–674.
- Myler, P. J., Stacy, R., Stewart, L., Staker, B. L., Van Voorhis, W. C., Varani, G. & Buchko, G. W. (2009). *Infect. Disord. Drug Targets*, **9**, 493–506.
- Patil, H. G., Gundavda, M., Shetty, V., Soman, R., Rodrigues, C. & Agashe, V. M. (2016). *J. Orthop.* **13**, 40–42.
- Poe, R. H., Vassallo, C. L. & Domm, B. M. (1971). *Am. Rev. Respir. Dis.* **104**, 427–431.
- Serbzhinskiy, D. A., Clifton, M. C., Sankaran, B., Staker, B. L., Edwards, T. E. & Myler, P. J. (2015). *Acta Cryst.* **F71**, 594–599.
- Stacy, R., Begley, D. W., Phan, I., Staker, B. L., Van Voorhis, W. C., Varani, G., Buchko, G. W., Stewart, L. J. & Myler, P. J. (2011). *Acta Cryst.* **F67**, 979–984.
- Studier, F. W. (2005). *Protein Expr. Purif.* **41**, 207–234.
- Velasco-García, R., Zaldívar-Machorro, V. J., Mújica-Jiménez, C., González-Segura, L. & Muñoz-Clares, R. A. (2006). *Biochem. Biophys. Res. Commun.* **341**, 408–415.
- Veluthat, C., Venkatnarayan, K., Padaki, P. & Krishnaswamy, U. M. (2021). *BMJ Case Rep.* **14**, e242499.
- Winn, M. D., Ballard, C. C., Cowtan, K. D., Dodson, E. J., Emsley, P., Evans, P. R., Keegan, R. M., Krissinel, E. B., Leslie, A. G. W., McCoy, A., McNicholas, S. J., Murshudov, G. N., Pannu, N. S., Potterton, E. A., Powell, H. R., Read, R. J., Vagin, A. & Wilson, K. S. (2011). *Acta Cryst.* **D67**, 235–242.